euronoise

Design of a phase array ultrasonic sensor using vibration decoupled concept

Chia-Yu Lin[a], Chih-Chiang Cheng[a], Wen-Jong Wu[b], Chuin-Shan Chen[c], Jay Shieh[d] and Chih-Kung Lee[a]

[a]National Taiwan University, Rm.433, Institute of Applied Mechanics, No.1, Sec.4, Roosevelt Rd., 10617 Taipei, Taiwan
[b]Department of Engineering Science and Ocean Engineering, National Taiwan University, Rm.433, Institute of Applied Mechanics, No.1, Sec.4, Roosevelt Rd., 10617 Taipei, Taiwan
[c]Department of Civil Engineering, National Taiwan University, Rm.433, Institute of Applied Mechanics, No.1, Sec.4, Roosevelt Rd., 10617 Taipei, Taiwan
[d]Department of Material Science and Engineering, National Taiwan University, Rm.433, Institute of Applied Mechanics, No.1, Sec.4, Roosevelt Rd., 10617 Taipei, Taiwan
cylinx@mems.iam.ntu.edu.tw

Abstract

Phase array ultrasonic sensors have been used widely to generate higher directional radiating patterns where piezoelectric units are sparsely distributed in space. In this study, we present a novel design of a phase array ultrasonic sensor based on the concept of vibration decoupling. Decoupling is usually achieved by careful design of a source aperture, which allows piezoelectric units to be tightly located in the same structure. Our phase array sensor design was based on a cylinder with a dumbbell shape groove to decouple the vibration. A finite element method was used to optimize the design. Two piezoelectric discs were adhered to the bottom plate of the sensor whereby a desirable wave generation and detection were controlled adaptively. By electrical steering, the sensor was thus able to operate in a dipole mode. Prototypes of the sensor were made and experimental work was conducted to verify the simulation results.

1 Introduction

Ultrasonic transducers, which are used for distance detection, have been developed for over several decades and have been applied to various fields. Recently, distance detection has become an important feature for driving safety. For this reason, an ideal ultrasonic transducer should be able to generate an anisotropic beam pattern in a far field to eliminate receiving the noise reflected from the ground. In this way, a structure can receive the reflected waves as a sensor. However, as detailed in past literature, it is difficult to generate a pure anisotropic beam pattern with an ultrasonic transducer. [1-4]

A phase array provides a flexible and extensive application to the automotive industry. Its disadvantage is that vehicles cannot be attractively designed if many ultrasonic transducers are located on the bumper. Rapps et al. proposed a kind of transducer which contains multiple dispositions of piezo-oscillators in a one-vibration structure that can generate an anisotropic far-field beam pattern [5]. Our study incorporates the concept of a phase array to improve the anisotropic beam pattern.

In addition, our study adopts the concept of decoupled vibration in a transducer and then controlling the input phase difference to generate a far-field anisotropic beam pattern. Since the vibrational plate of a transducer has a very complex boundary, we adopted a finite element method to analyze the vibration mode so that we could obtain a decoupled dual source in the transducer. Consequently, we attached two piezoelectric actuators (lead zirconium titanate, i.e., PZT) to the vibration-decoupled structure and drove signals with different phases to obtain the specific far-field beam pattern.

2 Theory

2.1 Vibration of a plate

The information of each source such as mode shape, velocity, and displacement, can be found from the following equation of motion for a plate [6],

$$\nabla^4 u + \frac{3\rho(1-\nu^2)}{h^2 E}\frac{\partial^2 u}{\partial t^2} = 0, \qquad (1)$$

where ρ is the density of the material, ν the Poisson's ratio, E the modulus of elasticity, and h the half-thickness of the plate. From the governing equation, we can see that the rigidity of the plate is dependent on the geometric configuration. Moreover, the boundary condition affects the aperture function at the vibration source. As a result of the diffraction theory, the far-field beam pattern is related to the aperture function, which can be correlated to the boundary and rigidity of the plate.

2.2 Radiation beam pattern in a far field

According to the Huygens-Fresnel principle, a vibration plate generates a sound wave in a far field which is an integral of each infinitesimal simple source on the vibration plate. The beam pattern in the far field can be expressed as the same form as a Rayleigh integral which is [7],

$$p(r,\theta,\phi,t) = j\rho_0 c\frac{k}{2\pi}\frac{e^{j(\omega t-kr)}}{r}\times \iint_S U(\xi,\eta)e^{jk(\xi\sin\phi\cos\theta+\eta\sin\phi\sin\theta)}d\xi d\eta, \qquad (2)$$

where $\rho_0 c$ is the acoustic impedance, k the wave number, ω the angular frequency, λ the wavelength, θ the azimuthal angle, φ the polar angle, r the distance from the source to the observation position, and $U(\xi,\eta)$ the magnitude of the distribution of speed on the source plane. Under a steady state condition, the speed distribution was relative to the distribution of displacement on the source plane.

2.3 Simulation and analysis

Because of the constraint of the sensor size, a trade-off between the source level and the beam pattern results from the inevitability for the two adjoining sources in a single enclosure. In such a case, for the design of a vibration decoupled ultrasonic sensor, it is required that the tractions on one side of the outer wall do not lead to a bending effect at the opposite side of the structure. Therefore, the structure should have a strong outer wall to resist the tractions forced on it. It will also require a small channel between the two sources to isolate the vibration coupling between the two sources, rather than a wall to prohibit the vibration between the two adjoining sources (see Fig. 1).

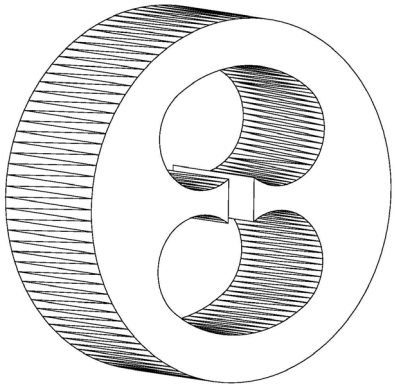

Fig. 1. Structure of the transducer.

In consequence, no analytic solution about the displacement can be seen in Eq. (1) due to the complex boundary condition of the structure of the transducer. Only by adopting a finite element method can we obtain the distribution of displacement. A harmonic response analysis in a finite element method was used to solve the time-dependent equation of motion of a linear structure and with steady-state vibration. As for symmetry, it was possible to build a half structure to reduce the calculation time. From Eq. (2), we can see that a far-field beam pattern is highly dependent on the operating frequency of the sensor. In order to study the design parameters, the diameter of the sensor was fixed at 23mm and the operating frequency held constant at 40 kHz.

2.4 Interference of waves from the two sources

The complex pressure amplitude of the outgoing wave in Eq. (2) can be reduced by the following expression,

$$P = \frac{A}{r} e^{j(\omega t - kr)}. \qquad (3)$$

The two point sources are located at $+d$ and $-d$ on the *z-axis* and the grazing angle θ with respect to the *x-axis* (see Fig. 2).

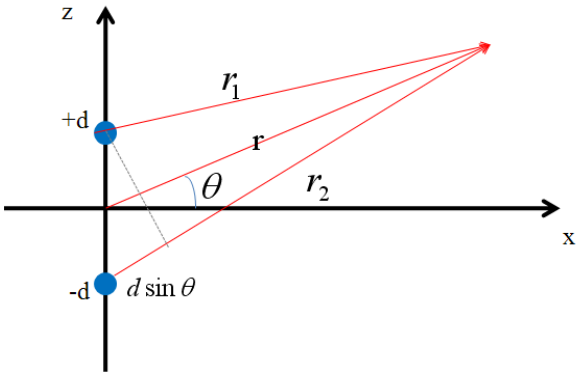

Fig. 2. Geometry of the two sources used for calculating the acoustic field point.

Therefore, the total complex amplitude from the two point sources can be expressed as follows,

$$P = A\left(\frac{1}{r_1} e^{-jkr_1} + \frac{1}{r_2} e^{-jkr_2}\right) e^{jwt}. \qquad (4)$$

When the distance r is much larger than $d \sin\theta$, Eq. (4) can be approximated to Eq. (5) as follows [8],

$$p(r,\theta,t) \approx \frac{2A}{r} \cos(kd \sin\theta) e^{j(\omega t - kr)}. \qquad (5)$$

Hence, in a Fraunhofer regime, the interference pattern can be calculated by $\cos(kd \sin\theta)$. The result of the beam pattern will also be the same as that of a one point source above the rigid boundary, which means that the product of a wave number k and distance d between the center and the source plays a major role on the beam pattern as shown in Fig. 3. When the product of the two factors is much smaller than 1, the two point sources can be replaced by one single point source [9]. When the path difference is an integral number of wavelengths, constructive interference can occur. In contrast, when the path difference is an odd number of half wavelengths, destructive interference will instead take place [10]. Thus, we can also control the input phase between the two sources to bring the difference beam pattern to a Fraunhofer regime condition.

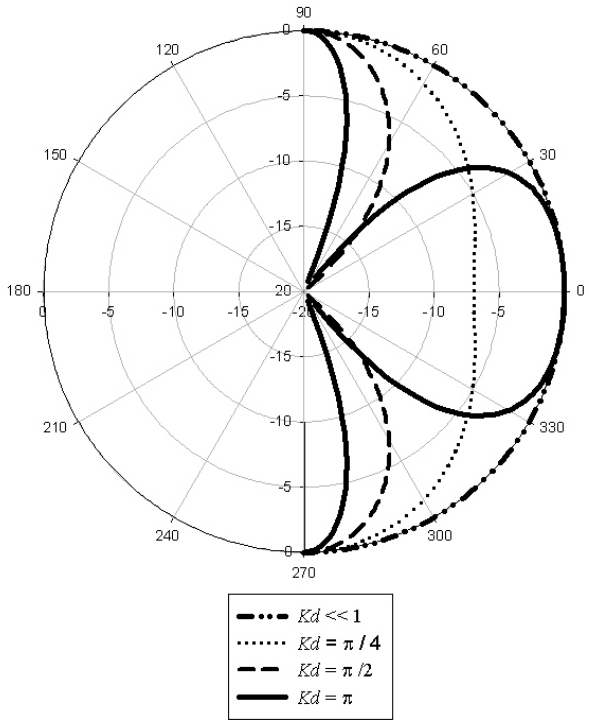

Fig. 3. Beam pattern of two point sources vibration in phase with various *kd*.

3 Experimental set-up

For measuring a Fraunhofer regime beam pattern, our experimental set-up was designed in a semi-anechoic environment to avoid reflected waves from complicated obstacles. The transducer was placed at a height of one meter above the ground to avoid receiving the wave reflection from the ground. A microphone was aligned to the acoustic axis of the transducer, and the distance between

the transducer and the microphone was set at one meter as required under a Fraunhofer regime. A Hewlett-Packard HP3245A generated the driving signal and controlled the phase difference. A G.R.A.S. 40BF (G.R.A.S. Sound and Vibration, Denmark) one-quarter inch standard microphone was connected to a B&K 2670 (Brüel & Kjær, Denmark) pre-amplifier to receive the acoustic waves generated by the transducer. For measuring the beam pattern of the transducer, the transducer was placed on a step motor stage which was controlled automatically to rotate from –90 degrees to +90 degrees. Thus, the beam pattern was determined by the relative orientation between the standard microphone and the transducer. The receiving signal was then amplified by the B&K 2670 and collected by a DAQ Card 6251 (National Instruments, USA). A LabVIEW program was then used for the automatic measurement. The sound pressure level was normalized with respect to the maximum pressure under the experimental set-up (see Fig. 3).

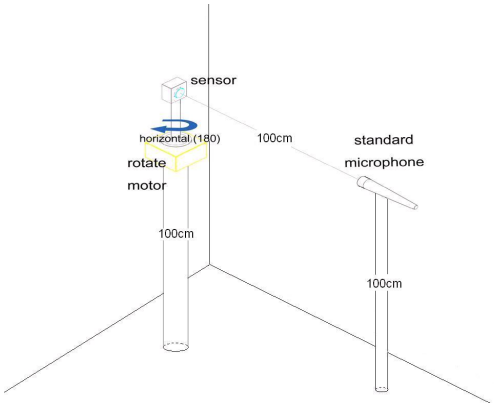

Fig. 3. Experimental set-up.

4 Results and Discussion

Fig. 4 demonstrates the optimal simulation results for the ultrasonic sensor under a resonant frequency of 40 kHz. The corresponding wavelength was 8mm, and the distance between the two adjoining sources was 9mm (ratio $d/\lambda = 0.5625$). By adopting a finite element method, the displacement at the centerline of the structure (Fig. 4) driven by one PZT can be seen in Fig. 5. The maximum normalized amplitude ratio of the two sources was 0.08. Accordingly, we made sure that one vibrating source did not affect the other.

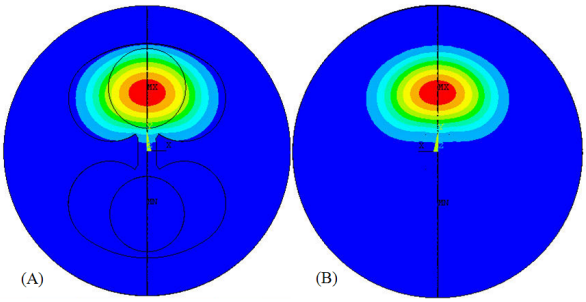

Fig. 4. Mode shape of the structure obtained by a finite element method: (A) top view, and (B) bottom view.

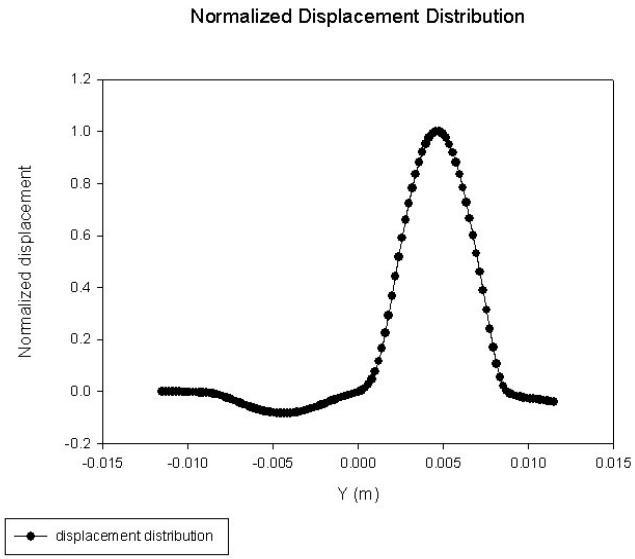

Fig. 5. Normalized displacement of the centerline of the structure.

The mode shape also obtained by a finite element method was in good agreement with that obtained by our experimental verifications. Fig. 6, which shows a picture taken after placing carbon powder on the vibrating plate of the sensor, implies that the vibration was successfully decoupled with the two sources.

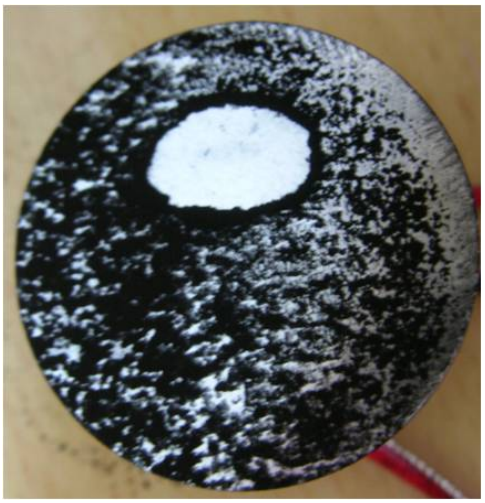

Fig. 6. Experimental result of the decoupled vibration.

We adopted a finite element method to obtain a normalized displacement of the centerline by driving two PZT actuators. By substituting a normalized displacement of the centerline into a simplified Fourier transform, we obtained a far-field beam pattern as seen in Fig. 7.

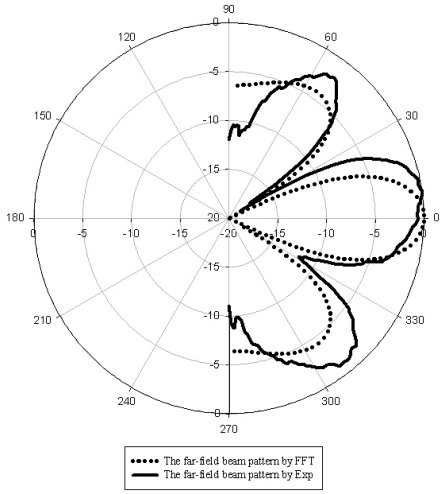

Fig. 7. Far-field beam pattern comparison between the FEM and experimental data.

The far-field logarithmic beam pattern obtained by our experimental set-up validates our simulation data. However, the beam pattern in a high spatial frequency possesses an inherent error using a Fourier transform [11]. In our case, the product of the wave number k and the distance d between the center and the source was 1.125π, under which the beam pattern is similar to the one under the product equaling to π, as seen in Fig. 3, which did not perfectly match Fig. 7 due to the fact that the vibration source in our case was not a point source.

To verify the electric steering by a phase delay between the two sources, two signals with various fixed phase delays were applied. The beam pattern as well as the numbers of lobes was altered by shifting the phase delay. There were three lobes when the two sources were driven in the phase, and the main lobe width was 30 degrees. The beam pattern rotated counter-clockwise with an increasing phase delay between the two sources. The lobe on the left increased gradually to the main lobe while the lobe on the right tended to fade away. When the phase delay reached 180 degrees, only two lobes still existed in the far-field beam pattern. When the phase delay was continuously increased, a new lobe on the right formed and the beam pattern would then revert back to its three original lobes (see Fig. 6).

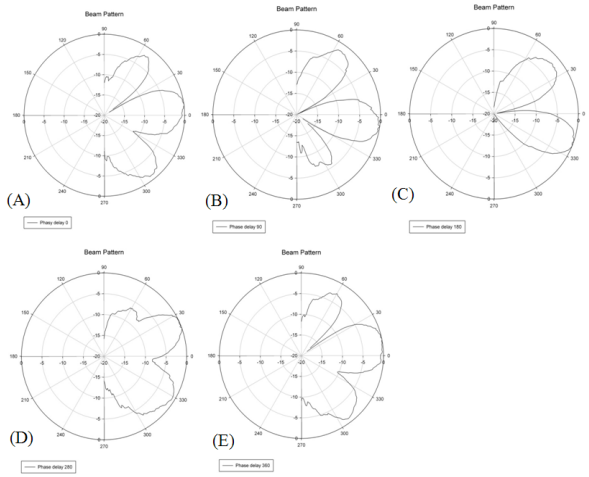

Fig. 6. Beam pattern of the phase delay at (A) 0 deg. (B) 90 deg., (C) 180 deg., (D) 280 deg., and (E) 360 deg.

5 Conclusions

We successfully designed a vibration decoupled structure in which a transducer can produce two independent but closely aligned sources. The resonant frequencies of the two vibration sources were the same, as a result of the symmetry of the structure. When the distance to be measured is short, we can actuate one PZT to generate ultrasonic waves, and use the other one to receive the reflected waves. Therefore, our newly designed transducer has no problems with reverberation during structural oscillation unlike traditional transducers. We found that the far-field beam pattern is dependent on the product of the wave number as well as the distance between the center and the source. Moreover, as a transmitter generates an ultrasonic wave that sweeps in space, the sweeping coverage can be controlled by input signals from the phase delay. In summary, our newly developed transducer can be expanded to have a wider applicability since the ultrasonic waves generated can go farther without the possibility of the waves being reflected from the ground.

References

[1] S.H. Li, "Ultrasound Sensor for Distance Measurement," United States Patent No. 6,181,645, Jan. 30 (2001).

[2] S.H. Li, "Ultrasound Sensor for Distance Measurement," United States Patent No. 6,370,086, Apr. 9 (2002).

[3] S. Amaike, and J. Ota, "Ultrasonic Sensor," United States Patent No. 6,250,162, June 26 (2001).

[4] S. Amaike, and J. Ota, "Ultrasonic Wave Transmitter/Receiver," United States Patent No. 6,593,680, July 15 (2003).

[5] P. Rapps, P. Knoll, F. Pachner, M. Noll, and M. Fischer, "Ultrasonic Transducer," United States Patent No. 5,446,332, Aug. 29 (1995).

[6] P.M. Morse, *Vibration and Sound*, 2nd Ed., McGraw-Hill Book Company, Inc., New York (1948).

[7] L. Rayleigh, *Theory of Sound*, 2nd Ed., Macmillan, London (1896).

[8] L.E. Kinsler and A.R. Frey, *Fundamentals of Acoustics*, 2nd Ed., John Wiley & Sons, Inc., New York (1962).

[9] M.C. Junger and D. Feit, *Sound, Structures, and Their Interaction*, 2nd Ed., MIT Press, Massachusetts (1986).

[10] K.U. Ingard, *Fundamentals of Waves & Oscillations*, Cambridge University Press, Cambridge (1988).

[11] J.W. Goodman, *Introduction to Fourier Optics*, McGraw Hill, New York (1995).

ACKNOWLEDGEMENT

The authors gratefully acknowledge the funding support of Eleceram Technology Co. Ltd., AdvanceWave

Technologies, Inc., the Materials and Chemical Engineering Research Laboratory of the Industrial Technology Research Institute (ITRI), and National Science Council of Taiwan under Contract No. NSC95-2622-E-002-0003. The continuous support and discussions of the Tung Thih Enterprise Co. Ltd, Taiwan is also greatly appreciated.